applied sciences

MDPI

Communication

Numerical Study on a Diesel/Dissociated Methanol Gas Compression Ignition Engine with Exhaust Gas Recirculation

Bo Li, Yihua Chen, Fei Zhong * and Hao Xu

School of Mechanical Engineering, Hubei University of Technology, Wuhan 430068, China; libo@hbut.edu.cn (B.L.); 102110114@hbut.edu.cn (Y.C.); haoxu42@outlook.com (H.X.)
* Correspondence: zhong_fei_hbut@163.com; Tel.: +86-15807163787

Abstract: Hydrogen is the most promising alternative fuel in the field of engines. Exhaust heat-assisted methanol dissociation is an attractive approach for generating hydrogen. In this work, simulations are conducted on a compression ignition engine fueled with different proportions of diesel-dissociated methanol gas (DMG) blends at intermediate engine speed, full load, and 0% EGR ratio. The results reveal that the indicated thermal efficiency and indicated mean effective pressure are greatly enhanced, combustion efficiency is increased, and regular emissions of CO, HC, and soot are reduced, while NOx emissions are reduced with increased DMG substitution. In addition, a simulation is conducted at an intermediate engine speed, full load, 15% DMG substitution ratio, and varying EGR ratios of 0–20%. The results indicate that the dual-fuel engine outperforms the original engine with respect to power, fuel economy, and regular emissions, once an optimal EGR rate is adopted.

Keywords: numerical study; dissociated methanol gas; compression ignition engine; substitution; exhaust gas recirculation; emission

check for updates

Citation: Li, B.; Chen, Y.; Zhong, F.; Xu, H. Numerical Study on a Diesel/Dissociated Methanol Gas Compression Ignition Engine with Exhaust Gas Recirculation. *Appl. Sci.* **2023**, *13*, 9612. https://doi.org/10.3390/app13179612

Academic Editor: Aliaksandr Shaula

Received: 27 June 2023
Revised: 11 August 2023
Accepted: 21 August 2023
Published: 25 August 2023

Copyright: © 2023 by the authors. Licensee MDPI, Basel, Switzerland. This article is an open access article distributed under the terms and conditions of the Creative Commons Attribution (CC BY) license (https://creativecommons.org/licenses/by/4.0/).

1. Introduction

Rapid development of the world economy brings a growing demand for transportation. Diesel engines have become the primary power source for surface transport due to their high thermal efficiency. However, their wide application is limited by high emission levels and high fuel consumption. In order to address the environmental pollution and energy crisis caused by diesel engines, alternative fuels are considered to be effective solutions. In the past decade, various types of alternative engine fuels such as hydrogen (H_2), dimethyl ether (DME), alcohols, biofuels, compressed natural gas (CNG), liquefied petroleum gas (LPG), and some synthetic fuels have been extensively investigated. Among these candidates, hydrogen stands out as the most promising alternative fuel. The high burning rate of hydrogen improves the in-cylinder combustion process, while its wide combustion limit extends the lean limit of engine operation. Additionally, the only product of hydrogen combustion is water, which effectively reduces harmful emissions [1,2]. Thus, hydrogen is strongly encouraged in the field of internal combustion engines.

However, compression ignition (CI) of pure hydrogen is challenging due to its high auto-ignition temperature, which prevents its application in unmodified diesel engines. As a result, researchers have favored the use of diesel-hydrogen blends instead of pure hydrogen. The performance and emission characteristics of CI engines fueled with hydrogen-diesel blends have been extensively investigated. Ghazal [3] reported a 14% increase in engine power at high engine speeds and a 70% increase in engine power at high air-fuel ratios when hydrogen addition reached 40%. Qin et al. [4] investigated the combustion characteristics of a hydrogen-diesel dual-fuel engine and observed that as the hydrogen substitution rate increased, the heat release rate (HRR) and thermal efficiency increased simultaneously. Liew et al. [5] examined the effect of hydrogen addition on engine combustion and revealed a significant decrease in combustion duration through hydrogen

enrichment. Shigeru Miyamoto et al. [6] stated that the introduction of hydrogen led to an increase in NOx emissions. Kumar et al. [7] proposed a combustion model to predict the emissions of a diesel-hydrogen dual-fuel engine and achieved good agreement between simulation and experimental data across various operating conditions, thus ensuring accurate predictions. Ramsay et al. [8] conducted a numerical study of a diesel-hydrogen dual-fuel CI engine and showed that an optimized injection strategy could improve the thermal efficiency of a dual-fuel engine without worsening the emissions.

In addition to the hydrogen substitution ratio, exhaust gas recirculation (EGR) can significantly influence the in-cylinder composition. Loganathan et al. [9] examined a hydrogen-diesel direct injection (DI) engine with EGR and observed that increasing the EGR ratio led to higher peak HRR, combustion duration, and cyclic pressure fluctuation. Nag et al. [10] explored a hydrogen-diesel dual-fuel CI engine by varying the engine load, fuel composition, and EGR ratio. The results showed that the engine emissions were reduced by adjusting the EGR rate in dual-fuel mode. Wu et al. [11] simultaneously tuned the intake air temperature, fuel composition, and EGR ratio of a hydrogen-diesel engine by employing the classical Taguchi method. Through this approach, they were able to identify an optimal combination of parameters and achieved advancements in emissions, brake specific fuel consumption (BSFC), and brake thermal (BTE) efficiency. Furthermore, a comparative experimental investigation was carried out on a hydrogen-diesel dual-fuel engine, with variations in engine loads, EGR ratios, and intake air boosting conditions [12]. The results indicated that an appropriate level of hydrogen addition considerably mitigated both NOx and particulate emissions.

Based on previous research, the addition of hydrogen to diesel offers significant advantages in terms of enhancing performance and reducing emissions. However, the widespread adoption of hydrogen is limited by its expensive storage costs. A possible solution is on-board generating of hydrogen-rich gas from other compounds through the recovery of exhaust heat [13]. The most commonly employed methods for on-board hydrogen production include steam reforming, autothermal reforming, catalytic dissociation, and partial oxidation. A comparative study of three on-board approaches for generating hydrogen, namely steam reforming, autothermal reforming, and partial oxidation from diesel fuel, was conducted by Chuahy and Kokjohn [14]. The results demonstrated that the adoption of all three methods could improve engine efficiency. Among the methods, steam reforming proved to be the most effective method, resulting in an 8% increase in global efficiency compared to the baseline. The enhancement achieved by autothermal reforming was slightly lower than that of steam reforming. In contrast, the global efficiency improvement from partial oxidation was significantly less compared to the other two methods. Sittichompoo et al. [15] studied hydrogen production methods from ammonia dissociation catalytic decomposition and ammonia reforming by recovering the exhaust heat from a gasoline direct injection (GDI) engine. The results indicated that different methods yielded similar improvements in fuel economy and CO_2 emissions.

The sources of on-board hydrogen production can be diverse. Coal, natural gas, methane, methanol, ethanol, gasoline, ammonia, biomass, and some other fuels have been utilized for hydrogen production. Methanol is the most commonly used feedstock for hydrogen production due to its abundant resources and relatively high hydrogen production rate. Two practical approaches for generating hydrogen from methanol are steam reforming and catalytic dissociation; both approaches are endothermic reactions and require external energy input. Engine exhaust gas energy can be recovered and used as a heat source. In terms of hydrogen yield, steam reforming produces more hydrogen than catalytic dissociation for the same mass of methanol, but it requires more reaction energy and additional water. In our latest study [16], a methanol catalytic dissociation system was successfully implemented in a spark-ignition gasoline engine.

The composition of syngas, which varies depending on the feedstock used for generating hydrogen, can have a significant impact on the performance and emissions of a diesel engine. In a study conducted by Sahoo et al. [17], a diesel engine was fueled with

three different syngas compositions under various loads. The results demonstrated that at higher loads, better performance was achieved with a decrease in the fraction of hydrogen (H_2), while higher levels of carbon monoxide (CO) and hydrocarbon (HC) emissions were observed with an increase in the CO fraction. Similar findings were reported by Bhaduri [18], who found that increasing the H_2/CO ratio in syngas led to reduced HC and CO emissions in an HCCI engine. Christodoulou and Megaritis [19] conducted experimental and numerical studies on a diesel engine fueled with a mixture of diesel, nitrogen (N_2), and syngas. The results revealed that the introduction of syngas + N_2 into the diesel fuel reduced nitrogen oxide (NOx), CO, and soot emissions under specific operating conditions, albeit increasing fuel consumption at all test points. Additionally, Karimkashi et al. [20] carried out a modeling study on the ignition characteristics of a hydrogen-methanol-diesel mixture. They reported that low and intermediate concentrations of hydrogen in the mixture had minor effects on the first and second stages of ignition delay times, while high concentrations of hydrogen significantly reduced the ignition delay. Furthermore, Chuahy and Kokjohn [21] suggested that a higher H_2/CO ratio in reformed fuel resulted in a shorter combustion duration and lower heat release during the reactivity-controlled compression ignition (RCCI) combustion process. These research findings indicate that the performance as well as the combustion and emission characteristics of an engine are influenced by changes in fuel composition.

The studies mentioned above have primarily focused on compression ignition (CI) engines fueled with diesel-hydrogen mixtures and diesel-steam reformed gas mixtures. However, there is limited research on CI engines fueled with a blend of diesel and methanol dissociation gas (DMG). In our previous investigation [16], the hydrogen content in DMG was between 60.7% and 64.8%, the CO content was between 19.1% and 23.1%, the methanol content was between 8.3% and 10.9%, and there was a small amount of by-products (carbon dioxide, methane, dimethyl ether, etc.) once the reaction temperature of 380–400 °C, the space velocity of 1.2–1.5/h, and a copper-based catalytic reactor were adopted. The changes in fuel composition and operation parameters may have had an impact on the engine working process. Consequently, in this study, we conduct a numerical investigation on a CI engine fueled with a blend of diesel and DMG at various substitution ratios and exhaust gas recirculation (EGR) rates. The objective is to explore the combination effects of DMG substitution ratio and EGR rate on the engine's performance, combustion, and emission characteristics.

2. Modeling and Validation

2.1. Engine Model

A DCI11 CI engine produced by Dongfeng motor corporation was employed for the numerical study. Its specifications are listed in Table 1.

The simulation study was conducted in CONVERGE package. The major models related to the CFD simulation are listed in Table 2. A Kelvin–Helmholtz Rayleigh–Taylor (KH-RT) model was employed to predict the primary and secondary breakups of the fuel droplet. The Frossling correlation method was used to simulate the droplet evaporation process. An RNG (Reynolds-averaged Navier–Stokes) k-ε model was employed to simulate turbulent flow. A no-time-counter (NTC) collision model was selected to describe the collision of the fuel droplets. A droplet drag model was established using a dynamic drag model, and the spray wall interaction was modeled using a rebound/slide model.

In many studies, n-heptane is commonly used as a surrogate for diesel due to its similar ignition characteristics [22,23]. Liu et al. [24] proposed a skeletal n-heptane mechanism that integrated a C0–C1 submodel, a C2–C3 submodel, and an enhanced low-temperature submodel. This model has been extensively validated under various conditions. Given its reliable performance, it was employed as the basic model in this study. The DMG mainly consisted of hydrogen, CO, and methanol. Its ignition and combustion could be predicted by using the C0–C1 submodel. To predict the emission of soot and NOx, the Hiroyasu-NSC soot model [25] and an extended Zeldovich skeletal model [26] were coupled with Liu's

model. The combustion of the diesel-DMG mixture was predicted in the SAGE chemistry solver, which was integrated into the CONVERGE package.

Table 1. The specifications of the test engine.

Parameter	Value
Number of cylinders	6
Cylinder bore (mm)	123
Stroke (mm)	156
Connecting rod length (mm)	228
Compression ratio	17.3
Combustion chamber geometry	ω
Top gap size (mm)	1
Swirl ratio	1.85
Intake valve closing (BTDC)	189
Exhaust valve opening (ATDC)	133
Number of nozzles	8
Injection angle (deg)	146
Injection cone angle (deg)	10
Diameter of the nozzle hole (mm)	0.158
Rated power/corresponding engine speed (kW/rpm)	330/1900

Table 2. Major models related to the CFD simulation.

Droplet Breakup Model	KH-RT
Droplet evaporation model	Frossling
Turbulent flow model	RNG k-ε
Droplet collision model	NTC
Spray wall interaction model	Rebound/slide
Droplet drag model	Dynamic drag
Chemistry model	SAGE

A 45° sector mesh was selected to reduce the computational cost. The base mesh was set as 4 mm. Additionally, an adaptive mesh refinement (AMR) algorithm was adopted to locally refine the meshing. The combustion chamber computational mesh at the top dead center (TDC) is depicted in Figure 1.

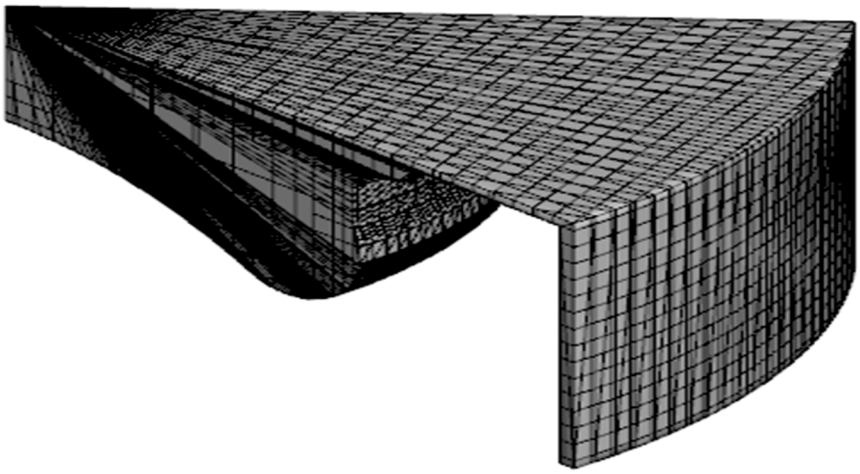

Figure 1. Computational mesh of the engine combustion chamber at the TDC.

2.2. Validation

The experimental data used for model validation came from the Huazhong University of Science and Technology Engine Research Laboratory. The operating conditions are listed

in Table 3. It is noted that the temperatures of the cylinder head, cylinder liner, and piston top were set as 593 K, 503 K, and 593 K, respectively.

Table 3. Operating conditions for the validation.

Parameter	Value
Engine speed (rpm)	1500
Load	100%
Injected mass (mg/cyc)	237
Injected pressure (MPa)	180
SOI (CA ATDC)	−5°
Injected duration (CA)	38°
Intake pressure (bar)	2.9
Intake pressure (K)	350
EGR ratio (%)	0

The comparison of the calculated and experimental data is shown in Figure 2. It can be observed that the experimental cylinder pressure is accurately predicted by the model. There is a slight overprediction of the simulated maximum HRR compared to the measured HRR. The discrepancy may be attributed to the differences between n-heptane fuel and diesel fuel. To improve the predictive accuracy, it is suggested that diesel surrogates should incorporate additional components such as toluene and cyclohexane [27]. Nevertheless, the deviation is acceptable, and this numerical model can be used for the numerical study of diesel-DMG dual-fuel engines.

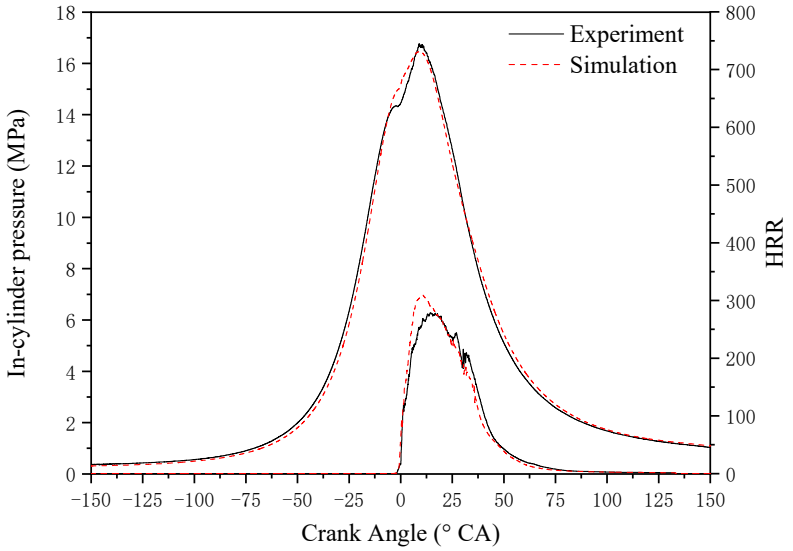

Figure 2. Model validation of in-cylinder pressure and HRR.

3. Results and Discussion

3.1. Definition of Dissociated Methanol Gas Substitution Ratio

In the simulations, the total energy is assumed to be constant, so:

$$E_{total} = M_m \cdot H_m + M_d \cdot H_d = M_{d0} \cdot H_d \quad (1)$$

In Equation (1), E_{total} is the total energy consumption rate of the original engine fueled with diesel; M_m and M_d are the mass consumption rates of methanol and diesel when the engine fueled with diesel-DMG mixtures, respectively; H_m and H_d are the low calorific values of methanol and diesel, respectively; M_{d0} is the consumed mass of diesel when the engine is fueled with neat diesel. Therefore, the DMG substitution ratio l is calculated as follows:

$$l = \frac{M_m \cdot H_m}{M_m \cdot H_m + M_d \cdot H_d} \quad (2)$$

According to experimental data, the cycle diesel injection quantity of the original engine is 237 mg/cyc at 1500 rpm and full load. For each substitution ratio, the diesel and methanol mass fraction can be calculated according to Equations (1) and (2). Thus, the DMG composition can be obtained when the methanol consumption is determined. In this study, the dissociation by-products were negligible since they were small in proportion. The fuel consumptions of different DMG substitution ratios are shown in Table 4.

Table 4. The fuel consumption per cycle results and DMG compositions at different substitution ratios.

Substitution Ratio	Diesel Consumption per Cycle (mg/cyc)	Methanol Consumption per Cycle (mg/cyc)	CH_3OH Mass in DMG (mg/cyc)	CO Mass in DMG (mg/cyc)	H_2 Mass in DMG (mg/cyc)
0%	237	0	0	0	0
10%	213.3	49.716	27.264	19.877	2.575
15%	201.45	74.574	40.897	29.815	3.863
20%	189.6	99.432	54.529	39.753	5.151

Since the simulations began at the IVO, the DMG-air mixture had already formed. The component of air should be considered. Therefore, the initial in-cylinder composition included N_2, O_2, CH_3OH, CO, and H_2. Their mass fractions are set in Table 5.

Table 5. The initial in-cylinder compositions at different substitution ratios.

Substitution Ratio	O_2 Mass Fraction	N_2 Mass Fraction	CH_3OH Mass Fraction	CO Mass Fraction	H_2 Mass Fraction
0%	23%	77%	0	0	0
10%	22.797%	76.319%	0.485%	0.354%	0.0458%
15%	22.692%	75.968%	0.735%	0.536%	0.0694%
20%	22.590%	75.626%	0.979%	0.735%	0.0924

3.2. Effects of Different DMG Substitution Ratiso on the Dual-Fuel Engine

In this section, simulations were conducted at an engine speed of 1500 rpm, full load, and the DMG substitution ratio ranged from 0% to 20%. The operating conditions are detailed in Table 3. The analysis focuses on evaluating the performance as well as the combustion and emission characteristics of the dual-fuel engine system.

3.2.1. Performance Characteristics

The indicated thermal efficiency (ITE) and the indicated mean effective pressure (IMEP) are two critical indicators used to evaluate engine performance. The simulated ITE and IMEP results of the dual-fuel engine for different DMG substitution ratios are presented in Figure 3; both ITE and IMEP demonstrate an increase as the DMG substitution ratio increases. The ITE is 42.0% for the diesel engine, and it increases to 46.1% when the DMG substitution ratio increases to 20%. The growth is approximately 4%. The IMEP is 2.29 MPa for the diesel engine, and it increases to 2.50 MPa when the DMG substitution ratio increases to 20%. The reasons for the improvement in engine performance can be attributed to the enhanced premixed combustion facilitated by the presence of hydrogen and CO in the DMG. This enhancement contributes to a more uniform and efficient combustion process. Additionally, methanol's relatively lower cost compared to diesel is advantageous in terms of reducing overall fuel expenses.

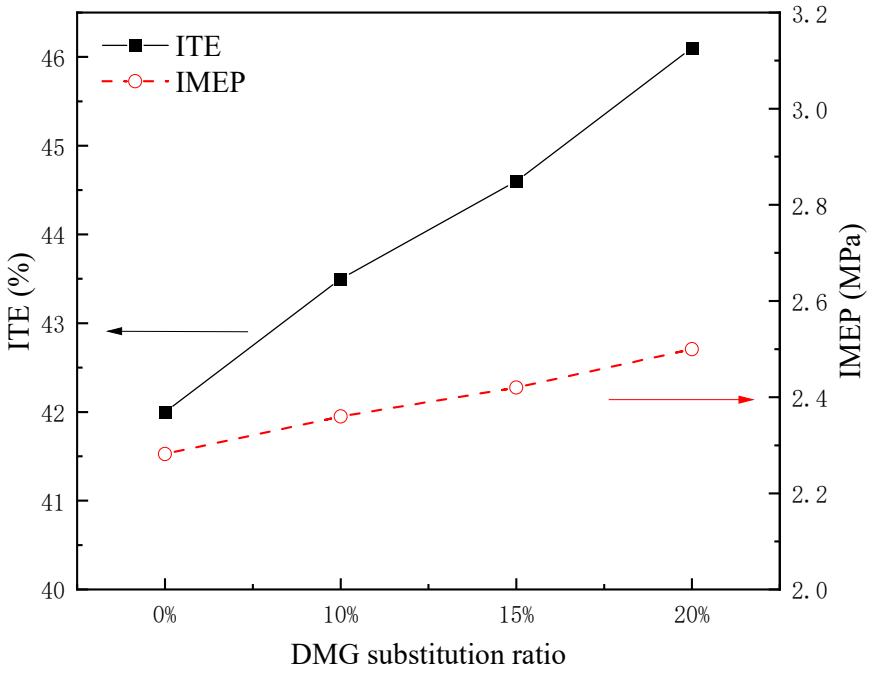

Figure 3. Effects of different substitution ratios on ITE and IMEP.

3.2.2. Combustion Characteristics

The effects of different DMG substitution ratios on in-cylinder combustion are depicted in Figure 4.

Figure 4a illustrates the impact of the DMG substitution ratio on the in-cylinder pressure of the dual-fuel engine. As shown in the figure, the peak in-cylinder pressure and the rate of pressure rise exhibit an increase with an increase in the DMG substitution ratio. Specifically, the original engine records a peak in-cylinder pressure of 16.32 MPa, occurring at 8.8° crank angle (CA). However, for a 20% DMG substitution ratio, the peak cylinder pressure rises to 19.74 MPa, marking a 21.96% increase. The corresponding crank angle is also delayed to 10.4° CA.

Figure 4b demonstrates the effects of different DMG substitution ratios on the in-cylinder average temperature of the blend combustion. In the figure, the peak temperature and the temperature rise rate increase as the DMG substitution ratio increases. The in-cylinder peak temperatures for the 0%, 10%, 15%, and 20% DMG substitution ratios are 1710.5 K, 1747.0 K, 17183.2 K, and 1824.9 K, respectively, and their corresponding crank angles are 41.7° CA, 37.1° CA, 34.6° CA, and 30.5° CA, respectively.

The increased in-cylinder pressure and temperature result from the main components of the DMG, i.e., hydrogen, CO, and gaseous methanol, which all have faster burning speeds and higher combustion temperatures than diesel. When the DMG substitution ratio increased, the premixed combustion was enhanced and promoted the isochoric combustion rate.

The impact of the DMG substitution ratio on combustion can be better understood by simulating the distribution of in-cylinder temperatures (the simulated temperature distribution for the crank angle is shown in Table A1 in Appendix A). The simulation results regarding temperature indicated that the incorporation of DMG had a significant positive impact on achieving more homogeneous combustion.

Figure 5a shows the heat release rate against crank angle for different DMG substitution ratios. It is observed that the maximum HRR increases as the DMG substitution ratio increases.

The combustion quality within the cylinder can be characterized by the parameters CA10-90 and CA50. CA10-90 represents the crank angle duration between 10% and 90% of the total fuel's heat release, while CA50 denotes the crank angle at which 50% of the

total fuel's heat release occurs. In Figure 5b, variations in CA10-90 and CA50 with the crank angle are depicted for different DMG substitution ratios. The figure illustrates that the addition of DMG leads to a reduction in both CA10-90 and CA50. This can be attributed to the enhanced premixing ratio resulting from the increased DMG content. The improved premixing promotes a higher combustion rate, ultimately leading to a shorter combustion duration.

(**a**)

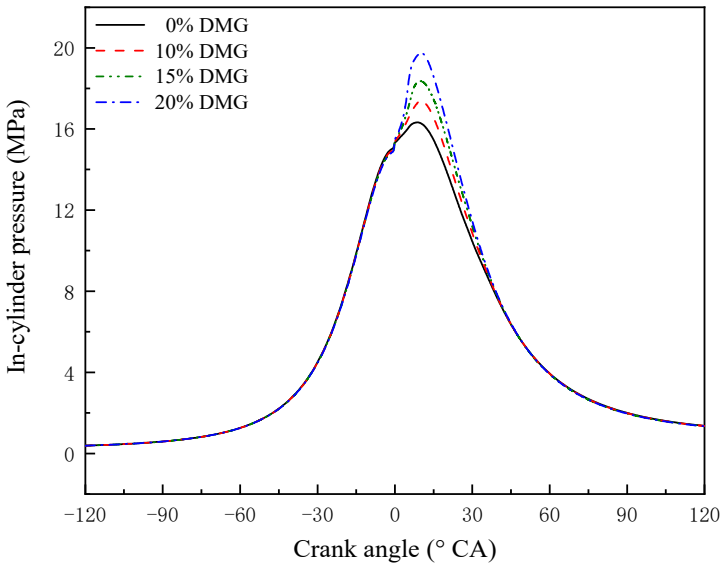

(**b**)

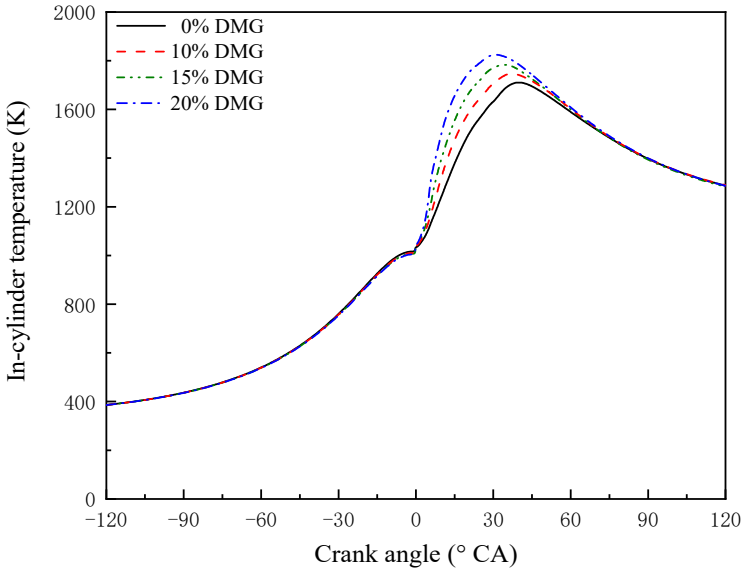

Figure 4. Effects of different DMG substitution ratios on in-cylinder combustion: (**a**) Pressure; (**b**) temperature.

(**a**)

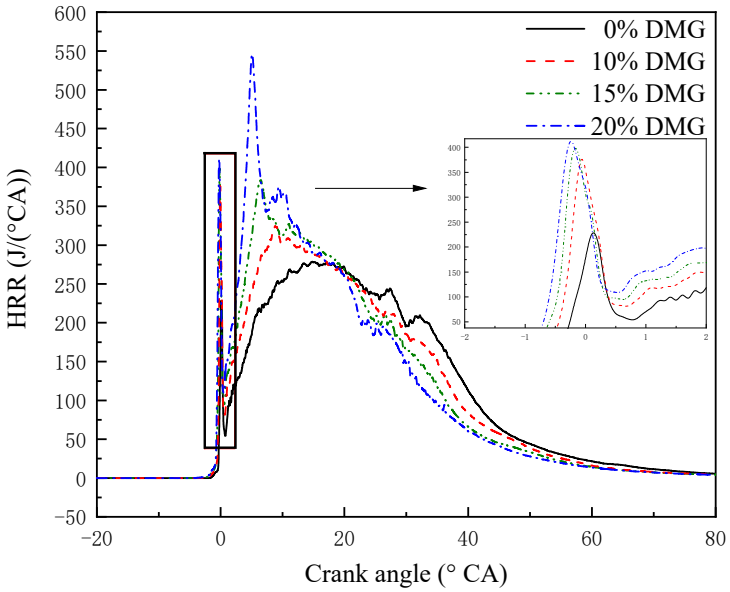

(**b**)

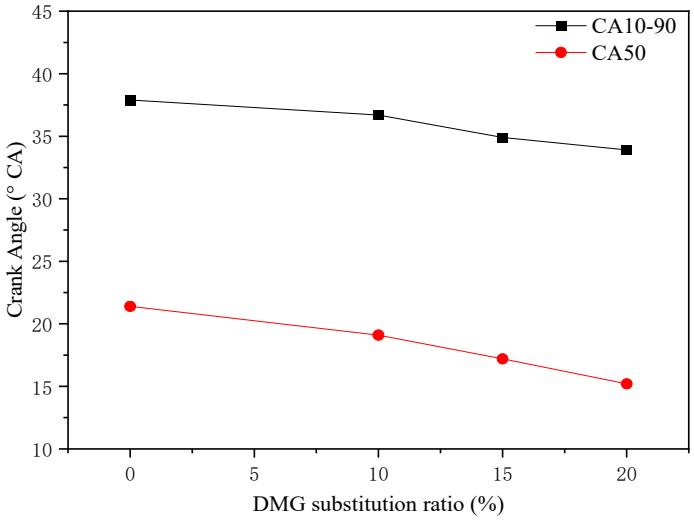

Figure 5. Effects of different DMG substitution ratios on HRR: (**a**) Profiles of HRR against crank angle; (**b**) CA10-90 and CA50.

3.2.3. Emission Characteristics

HC, CO, NOx, and soot are regulated emissions of a diesel engine. This section focuses on analyzing the effect of DMG addition on these emissions. Figure 6 illustrates the variations in emissions with different DMG substitution ratios.

It is observed from Figure 6 that CO emissions decrease gradually when the DMG substitution ratios range from 0% to 15%. However, when the DMG substitution ratio exceeds 15%, there is a sharp drop in CO emissions. The influence of DMG on CO emissions can be summarized in two aspects. First, CO is one of the main components of DMG; therefore, the addition of DMG can increase the CO content within the cylinder. Secondly, the addition of DMG raises the in-cylinder temperature and pressure, which facilitates the oxidation of CO to CO_2. At lower substitution ratios, the impact of CO oxidation is partially offset by the introduction of DMG, resulting in a slow decline of CO emissions.

However, at higher substitution ratios, the latter aspect becomes more prominent, leading to a significant reduction in CO emissions.

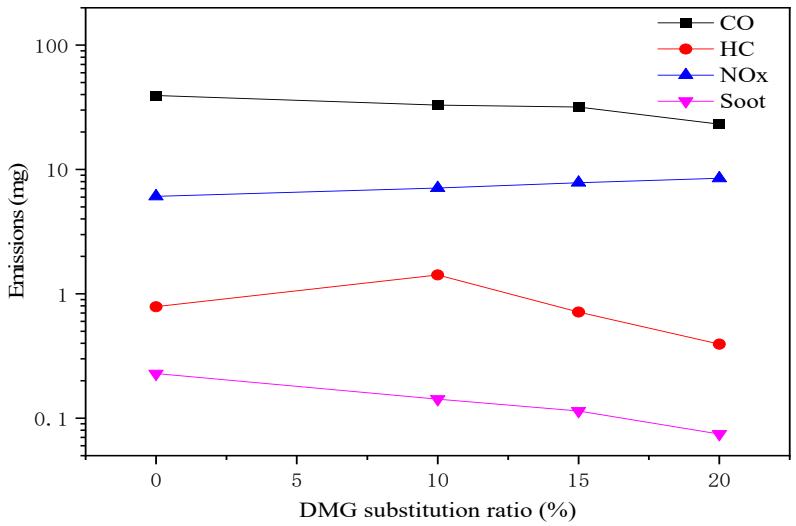

Figure 6. Effects of different DMG substitution ratios on emissions.

The red line in Figure 6 demonstrates the variations in HC emissions with different DMG substitution ratios. It is evident that HC emissions increase initially at low substitution levels and subsequently decrease at relatively higher substitution levels. Similar results have been reported in the literature [28]. The reasons can be summarized as follows: At low substitution levels, the high-temperature area within the combustion chamber is relatively small. Consequently, the mixture in the low-temperature area becomes difficult to ignite, leading to an increase in unburned HC emissions. Conversely, at higher substitution levels, the wider range of the high-temperature area aids in reducing HC emissions. Additionally, the quenching distances of hydrogen and CO (carbon monoxide) are shorter compared to those of diesel. This means that the flame can propagate closer to the cylinder wall and into crevices effectively, thereby promoting a more complete combustion process and reducing HC emissions more effectively.

The blue line in Figure 6 reveals that NOx emissions gradually increase with increased DMG fraction. The formation of NOx is highly dependent on local temperature and equivalence ratio. Temperature distributions and equivalent ratio distributions can be found in Figures A1 and A2 in Appendix A. It can be seen from the figures that the addition of DMG increases the in-cylinder temperature and makes the equivalence ratio distribution more homogenous, which provides sufficient conditions for generating NOx, resulting in higher NOx emissions.

Figure 6 also illustrates the variations in soot emissions with respect to the substitution ratio (see purple line). The figure indicates that the engine exhibits lower exhaust soot values when the DMG fraction is high. Comparing it with the original engine (0% substitution ratio), the reductions in soot emissions are 37.8%, 49.9%, and 67.4% for DMG substitution ratios of 10%, 15%, and 20% respectively. There are two reasons for the decline in soot exhaust. First, the carbon content in methanol is only 93.7% of that in n-heptane, assuming the calorific values of the two fuels remain the same. As a result, the carbon mass decreases with an increasing DMG fraction. Secondly, the methanol molecule contains an oxygen atom, and the relatively high temperature and oxygen-rich environment facilitate the oxidation of carbon soot. This oxidation process leads to a significant decrease in engine carbon soot emissions under the blending conditions.

The impact of the DMG substitution ratio on NOx and soot emissions can be better understood by simulating the distribution of NOx and soot (see Figures A3 and A4 in Appendix A).

3.3. Effect of EGR on the Dual-Fuel Engine

As discussed in the previous section, the addition of DMG significantly enhanced the power performance and fuel economy of the dual-fuel engine. Nevertheless, there were also increases in peak in-cylinder pressure, maximum pressure rise rate, and NOx emissions as the DMG substitution ratio increased. At a substitution ratio of 20%, the peak in-cylinder pressure reached approximately 20 MPa. Considering the overall performance as well as the combustion and emission characteristics, a DMG substitution ratio of 15% can be an optimal choice.

As an effective emission reduction technology, EGR has been widely applied to diesel engines. Since EGR can significantly influenced the in-cylinder composition and temperature, consequently impacting an engine's operational process, it is valuable to investigate the effect of EGR on a diesel-DMG dual-fuel engine. In this study, the EGR gas is considered to be a mixture of CO_2, H_2O, N_2, and O_2. Simulations were conducted at full load, an engine speed of 1500 rpm, a DMG substitution ratio of 15%, an intake temperature of 400 K, an intake pressure of 0.29 MPa, and varying EGR ratios from 0% to 20%. The initial intra-cylinder compositions were calculated for different EGR rates and are listed in Table A1 of Appendix A.

3.3.1. Performance Characteristics

Figure 7 shows the effects of EGR on the ITE and IMEP of the dual-fuel engine. It is evident that as the EGR rate increases from 0% to 20%, the ITE decreases from 42.3% to 39.4%, and the IMEP decreases from 2.33 MPa to 2.14 MPa. The results further reveal that, although EGR exhibits an adverse influence on both ITE and IMEP, the power output and fuel economy of the dual-fuel engine remain superior to those of the original engine as long as the EGR rate is below 20%.

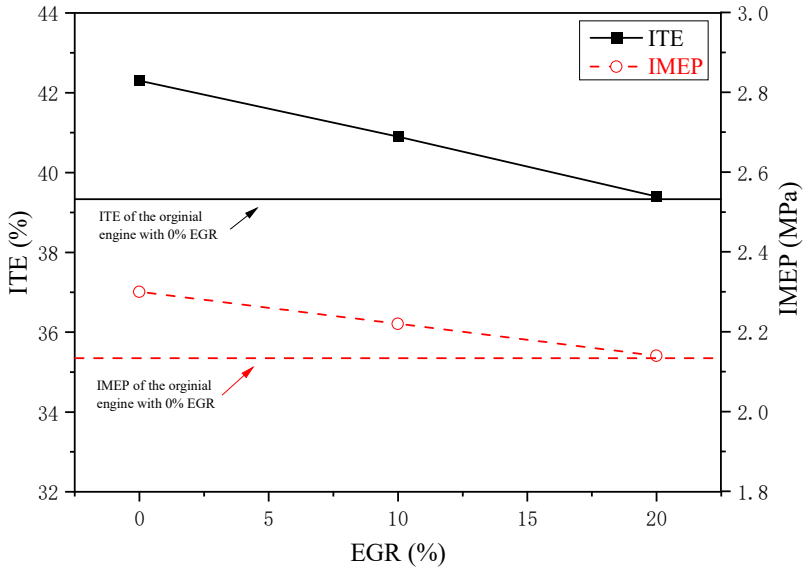

Figure 7. Effect of EGR rate on ITE and IMEP of the dual-fuel engine.

3.3.2. Combustion Characteristics

The effects of the EGR rate on in-cylinder combustion are depicted in Figure 8.

Figure 8a exhibits the influence of EGR rate on the in-cylinder pressure of the engine. As shown in the figure, an increase in the EGR rate causes a slight decrease in the maximum in-cylinder pressure. This can be attributed to the partial replacement of the inlet air by EGR gas, resulting in a reduction in oxygen concentration and a decrease in combustion efficiency. The deterioration of combustion subsequently leads to a decline in peak pressure. However, even with a 20% EGR rate, the peak in-cylinder pressure remains at 18.40 MPa, which surpasses the value of 16.32 MPa observed in the original engine fueled with pure

diesel. This suggests that the high combustion rate and oxygenation characteristics of DMG can overcome the deterioration caused by EGR.

(**a**)

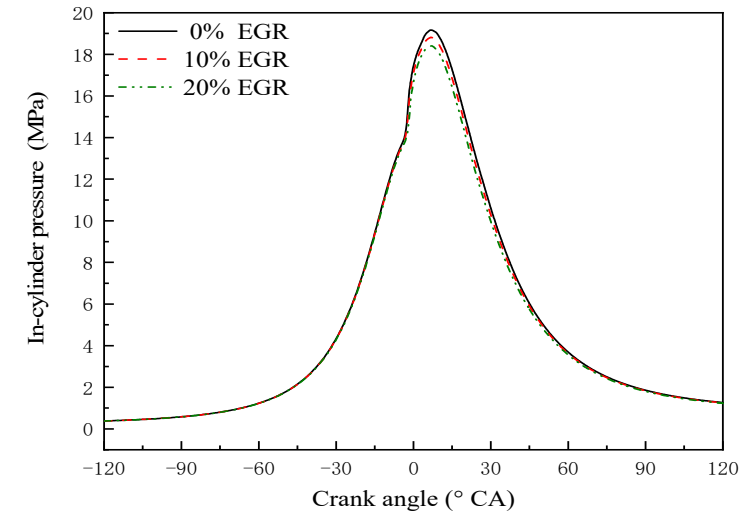

(**b**)

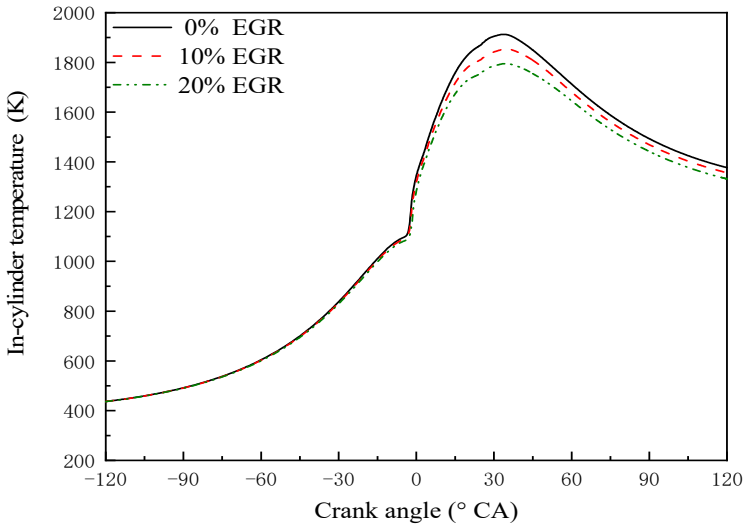

Figure 8. Effects of different EGR rates on in-cylinder combustion: (**a**) Pressure; (**b**) temperature.

Figure 8b demonstrates the effect of EGR rate on the in-cylinder average temperature of the dual-fuel engine. The in-cylinder temperature decreases with an increase in EGR rate. The decline in the in-cylinder temperature is mainly due to the fact that the recirculate gas is rich in CO_2 and H_2O; the two components have a relative higher specific heat capacity than air, which leads to a decrease in the in-cylinder temperature.

Figure 9 presents the relationship between HRR and crank angle. It is evident that the peak HRR diminishes and the average HRR slows down with an increase in the EGR rate. As discussed previously, the introduction of EGR results in decreases in in-cylinder pressure and temperature. This, in turn, reduces the oxidation reaction rate of the fuel, leading to a slight deceleration in the HRR. It is worth noting that the dual-fuel engine exhibits less sensitivity to EGR. This can be attributed to the presence of oxygen in the DMG, which helps to maintain the combustion process even with the introduction of EGR.

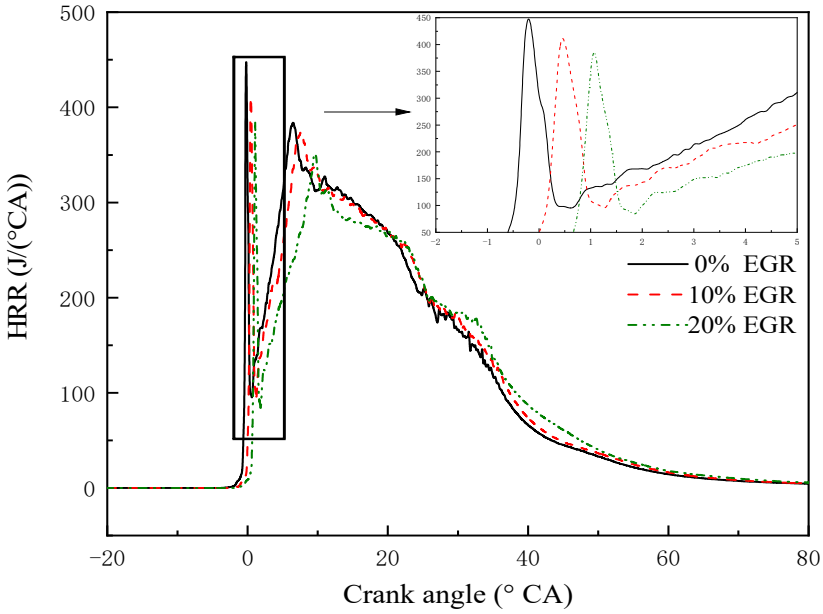

Figure 9. Effect of EGR rate on the HRR.

3.3.3. Emission Characteristics

The effects of EGR rate on emissions are depicted in Figure 10.

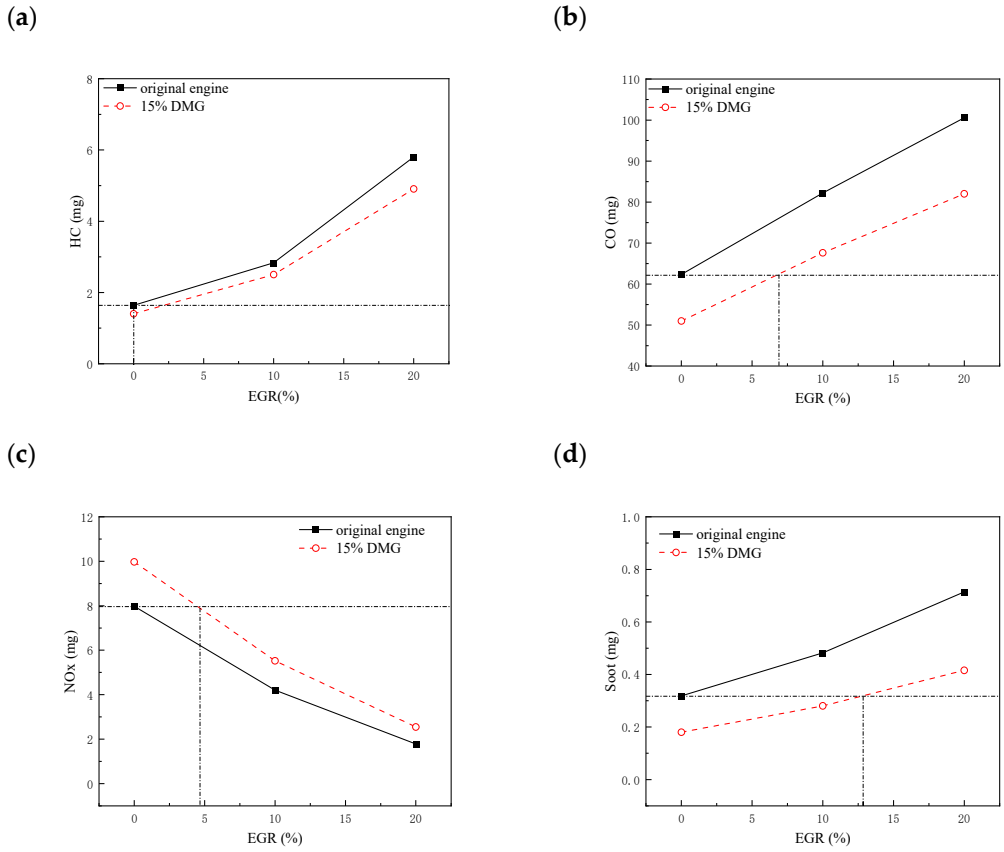

Figure 10. Effect of different EGR rates on emissions: (**a**) HC; (**b**) CO; (**c**) NOx; (**d**) Soot.

Figure 10a illustrates the effect of the EGR rate on HC emissions. It is evident that HC emissions increase as the EGR rate increases. This can be attributed to two factors. First, when EGR is applied, a portion of the intake air is replaced by recirculated gas, resulting in insufficient air for complete combustion. Secondly, an increase in the EGR rate leads to a reduction in the high-temperature area within the cylinder; both of these factors contribute an increase in to HC emissions. As discussed previously and depicted in Figure 10, there is minimal variation in HC emissions between a DMG substitution ratio of 0% and 15% at an EGR rate of 0%. Consequently, when the EGR rate is below 10%, the HC emissions of the original engine are similar to that of a 15% DMG substitution ratio, as demonstrated in Figure 10a.

Figure 10b displays the relationship between the EGR rate and CO emissions. It is evident that CO emissions increase as the EGR rate increases. This can be attributed to two factors. First, an increase in EGR rate leads to a reduction in the in-cylinder temperature, which inhibits the oxidation reaction of CO. Secondly, the dilution effect of EGR decreases the oxygen concentration in the intake air, further inhibiting the oxidation of CO. However, the addition of DMG enhances the oxidation reaction of CO due to its higher oxygen content. Therefore, at a lower EGR rate (less than 7%), the CO emissions of the dual-fuel engine are lower than that of the original engine without EGR. This indicates that the presence of DMG helps to mitigate CO emissions even with the application of EGR.

The variation in NOx emissions under the influence of EGR is displayed in Figure 10c. It is observed that NOx emissions drastically decline with an increase in EGR. For the dual-fuel engine with 20% EGR, NOx emissions declined 74.5% compared to that of the engine without EGR. This result strongly proves the efficiency of EGR on the inhibition of NOx generation. Additionally, at lower EGR rates (less than 4.9%), the NOx emissions of the dual-fuel engine are lower than those of the original engine without EGR.

According to the information in Figure 10d, there is a noticeable increasing trend in soot emissions as the EGR rate increases. This can be attributed to the fact that the introduction of recirculated gas reduces the oxygen concentration, temperature, and pressure inside the engine cylinder, creating a favorable environment for generating soot. However, when comparing the dual-fuel engine to the original engine without EGR, it is found that lower soot emissions can be achieved by the dual-fuel engine, particularly when the EGR rate is less than 13%. This is because the high temperature and rich oxygen content of DMG significantly improve the combustion environment. This compensates for the impact of EGR on soot emissions, resulting in lower soot levels even with the application of EGR.

In summary, the dual-fuel engine outperforms the original engine in power, fuel economy, as well as CO, NOx, and soot emissions, while it has similar HC emission levels as the original engine, once the DMG substitution ratio is 15% and the EGR rate is approximately between 5% and 7%.

4. Conclusions

This study proposes a multi-zone model to predict diesel/DMG combustion and regular emissions. Based on this model, numerical studies were conducted to investigate a CI engine fueled with different proportions of diesel-DMG blends at a constant engine speed of 1500 rpm and full load. In addition, the effects of EGR rate on performance, as well as the combustion and emission characteristics of a dual-fuel engine are also discussed. The major conclusions are summarized as follows:

- Increasing the energy share of DMG to 20% of the diesel input energy leads to an increase in ITE and IMEP. Compared to the original diesel engine, the increase is 9.7% for ITE and 9.2% for IMEP, indicating that DMG has the potential to improve engine power and fuel economy. Moreover, methanol has a lower price compared with diesel, which is beneficial for reducing total fuel cost.
- The addition of DMG increases in-cylinder pressure, average temperature, and HRR, makes the temperature distribution and local equivalence ratio more homogenous, and reduces both CA10-90 and CA50. These effects are because the main components

of DMG are hydrogen, CO, and gaseous methanol, which have fast burning speeds and high combustion temperatures, and therefore improve the combustion efficiency.

- For regular emissions, CO and soot emissions are reduced, HC emissions increase at low substitution levels and decrease at relative higher substitution levels, and NOx emissions decrease with an increase in the DMG substitution ratio. These trends are caused by the high combustion temperature and rich oxygen content of DMG.
- At 15% DMG substitution ratio, ITE and IMEP decrease with an increase in the EGR rate. However, the power and the fuel economy of the dual-fuel engine with less than 20% EGR rate are still higher than that of the original engine without EGR.
- The dilution effect and increased heat capacity caused by EGR have a negative effect on combustion efficiency and result in a decline in the maximum in-cylinder pressure, average temperature, and HRR. However, the high combustion speed and oxygenated nature of DMG partly compensate for this deterioration effect. Thus, the maximum in-cylinder pressure, average temperature, and HRR of the dual-fuel engine with lower EGR rates are still higher than that of the original engine.
- The application of EGR reduces the oxygen concentration, temperature, and pressure inside the engine cylinder. Therefore, CO and soot emissions of the dual-fuel engine increase, HC emissions remain at a similar level, and NOx emissions are drastically decreased with increasing EGR rate.
- The dual-fuel engine outperforms the original engine in power, fuel economy, and regular emissions once the DMG substitution ratio and EGR rate are optimized.

Overall, the addition of DMG in diesel improves engine performance and reduces HC, CO, and soot emissions. Although the presence of DMG leads to worsened NOx emissions, an optimal EGR rate can mitigate this effect. However, there are still unresolved issues. For instance, all the findings thus far were obtained under stable operating conditions. Further research is required to investigate conditions across a broad range of engine speeds and loads, incorporating diverse injection strategies.

Author Contributions: B.L., resources, writing—review and editing, supervision, funding acquisition; Y.C., investigation, validation, data curation; F.Z., writing—review, funding acquisition; H.X., conceptualization, visualization, writing—original draft, software. All authors have read and agreed to the published version of the manuscript.

Funding: This study was supported by the National Natural Science Foundation of China (Grant No. 52205147), the National Natural Science Foundation of China (Grant No. 52005168), and an open grant from the Hubei Provincial Key Laboratory of Modern Manufacturing Quality Engineering (KFJJ-2020009).

Institutional Review Board Statement: Not applicable.

Informed Consent Statement: Not applicable.

Data Availability Statement: The data used to support the findings of this study are available from the author upon request.

Conflicts of Interest: The authors declare no conflict of interest.

Appendix A

The following table and figures are those omitted from the main text for brevity.

Figure A1 illustrates the changes in in-cylinder temperature distribution at different crank angles, corresponding to various DMG substitution ratios. At 0° CA, a small area near the center of the cylinder head began to heat up. By 5° CA, the outer peripheral surface of the spray ignited, resulting in a rapid increase in temperature. As the DMG concentration in the cylinder increased with the substitution ratio, a greater number of flammable mixtures formed, leading to a broader high-temperature area. Additionally, the unburned gases surrounding the ignition region were heated, which, in turn, elevated the average in-cylinder temperature as compared with a lower substitution ratio. At 15°

CA, the fuel near the side wall ignited, causing a sharp rise in temperature. With an increase in the DMG substitution ratio, the efficiency of premixing improved, resulting in a more uniform distribution of temperatures. At a substitution ratio of 20%, temperatures above 1500 K were recorded throughout the cylinder. By 25° CA, the high-temperature region extended to the combustion chamber recess fillet. As the cycle progressed to 35° CA, residual fuel continued to burn. When a higher substitution ratio was utilized, the temperature distribution became more homogeneous, and the low-temperature region decreased in size.

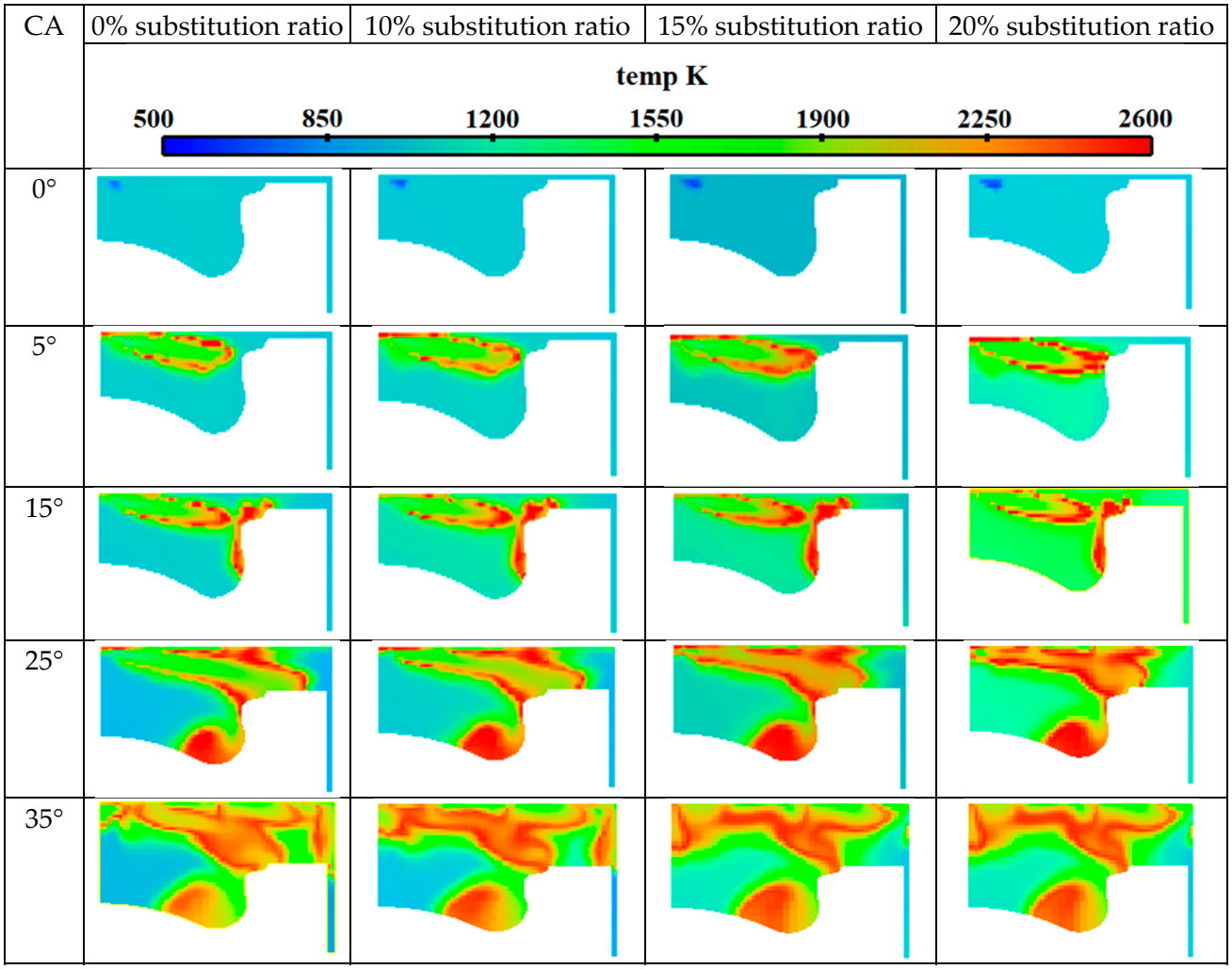

Figure A1. Effects of different DMG substitution ratios on the in-cylinder temperature distribution.

The equivalence ratio distribution for different substitution ratios is shown in Figure A2. It can be seen from the figure that the area of high equivalence ratio distributes mainly in the upper part of the combustion chamber around the spay, and the area of low equivalence ratio is found in the bottom region near the center axis. The simulation results indicate that the addition of DMG makes the equivalence ratio distribution more homogenous.

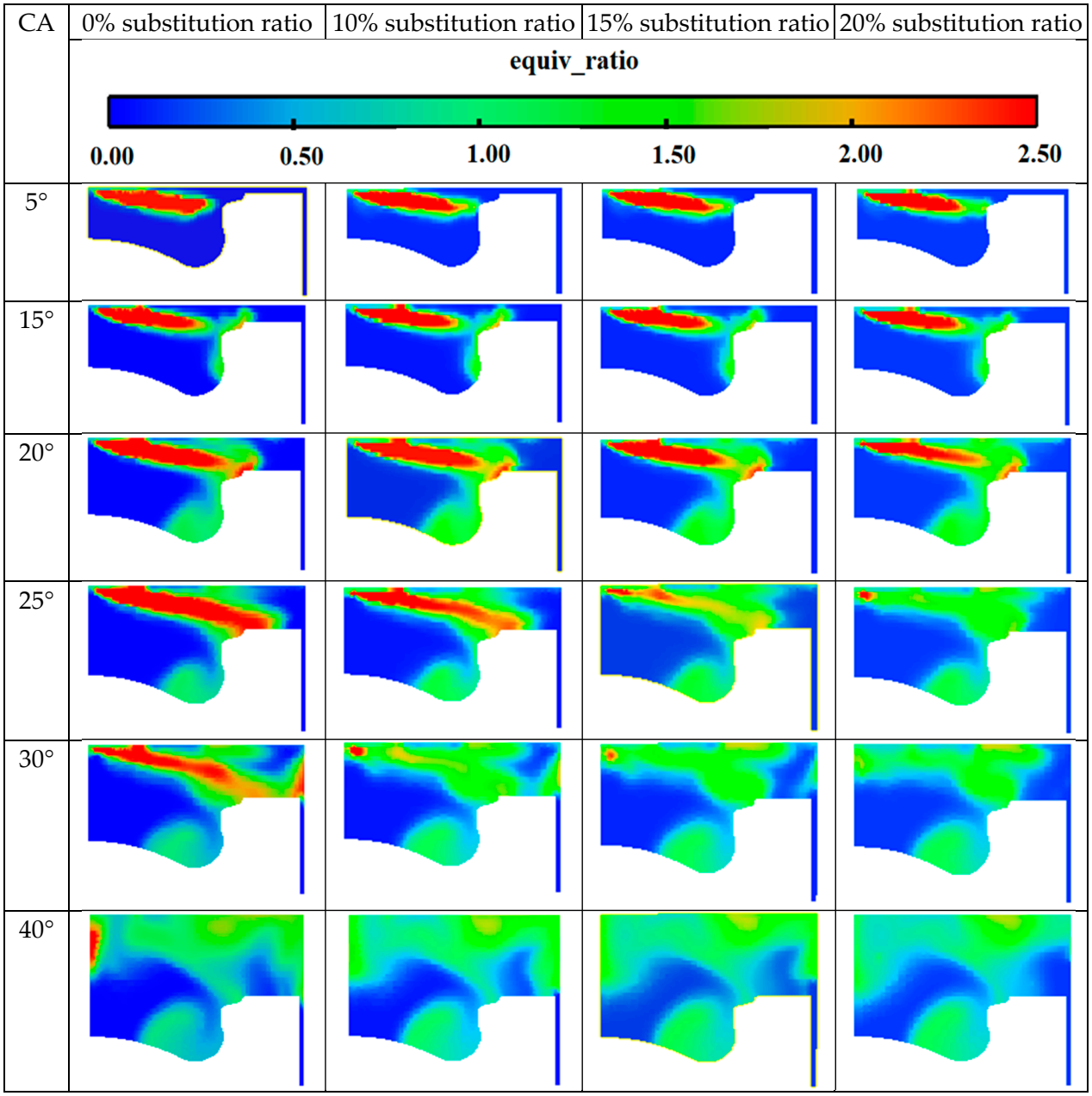

Figure A2. Effect of different DMG substitution ratios on the equivalence ratio distribution.

Figure A3 illustrates the variations in in-cylinder NOx distribution with respect to changes in crank angle and DMG fraction. The observations indicate that NOx is primarily generated in regions characterized by high temperatures and rich fuel conditions, which provide sufficient conditions for generating NOx. This region expands wider with increases in the DMG substitution ratio, resulting in a higher NOx emission.

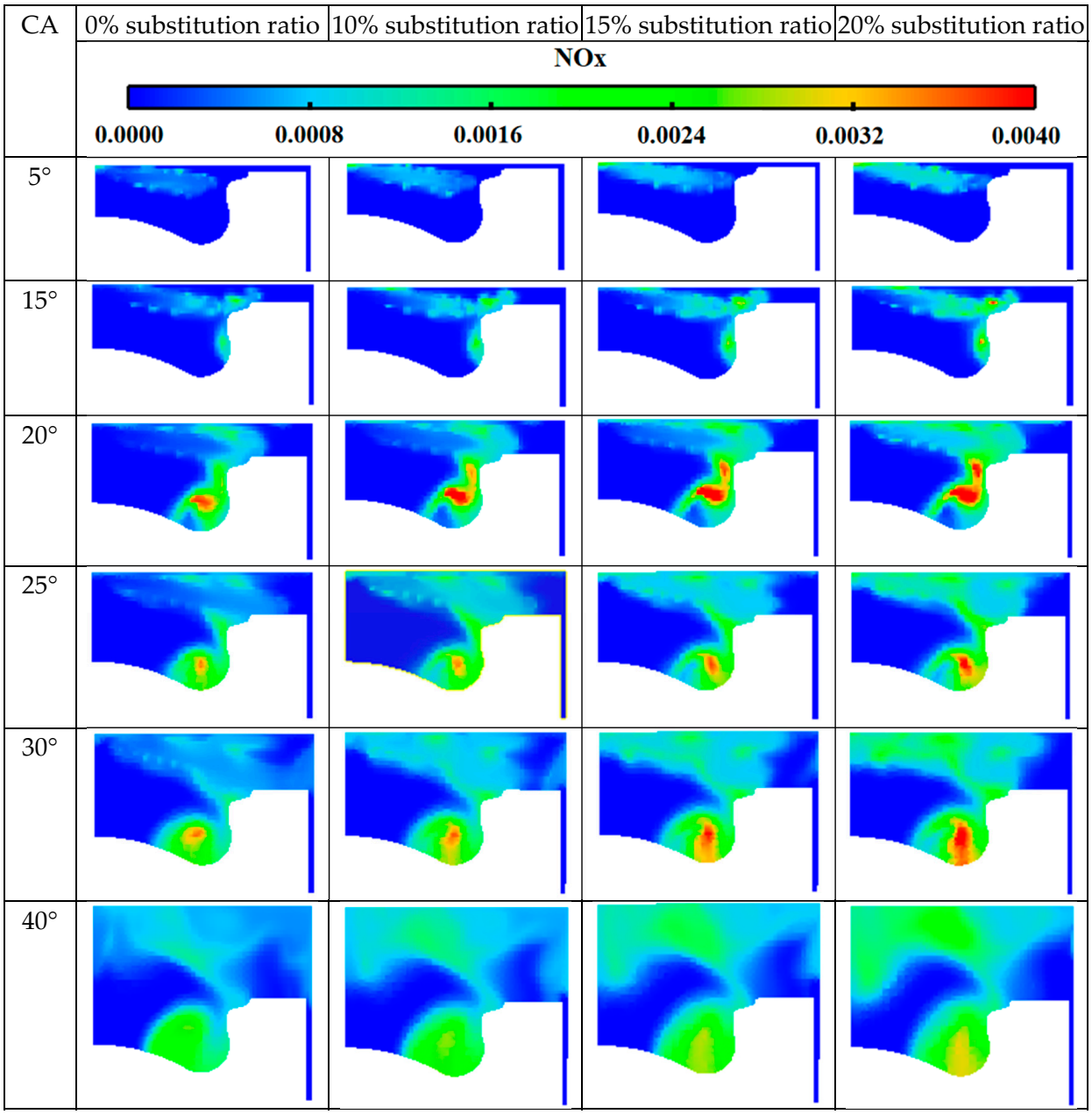

Figure A3. Effects of different DMG substitution ratios on the NOx distribution in mass.

Figure A4 exhibits the in-cylinder soot distribution concerning variations in crank angle and DMG fraction. The figure demonstrates that the total soot value increases between 5° CA and 30° CA and subsequently decreases. At 5° CA, first, soot emerges in the core of the spray. As the piston moves downward, soot becomes concentrated in the high equivalence ratio region. Around 30° CA, the soot concentration reaches its peak and is primarily distributed in the upper part of the combustion chamber. Afterward, the total soot value decreases due to the oxidation reaction. At 40° CA, some soot is still present near the center axis. In summary, the addition of DMG promotes the oxidation of soot.

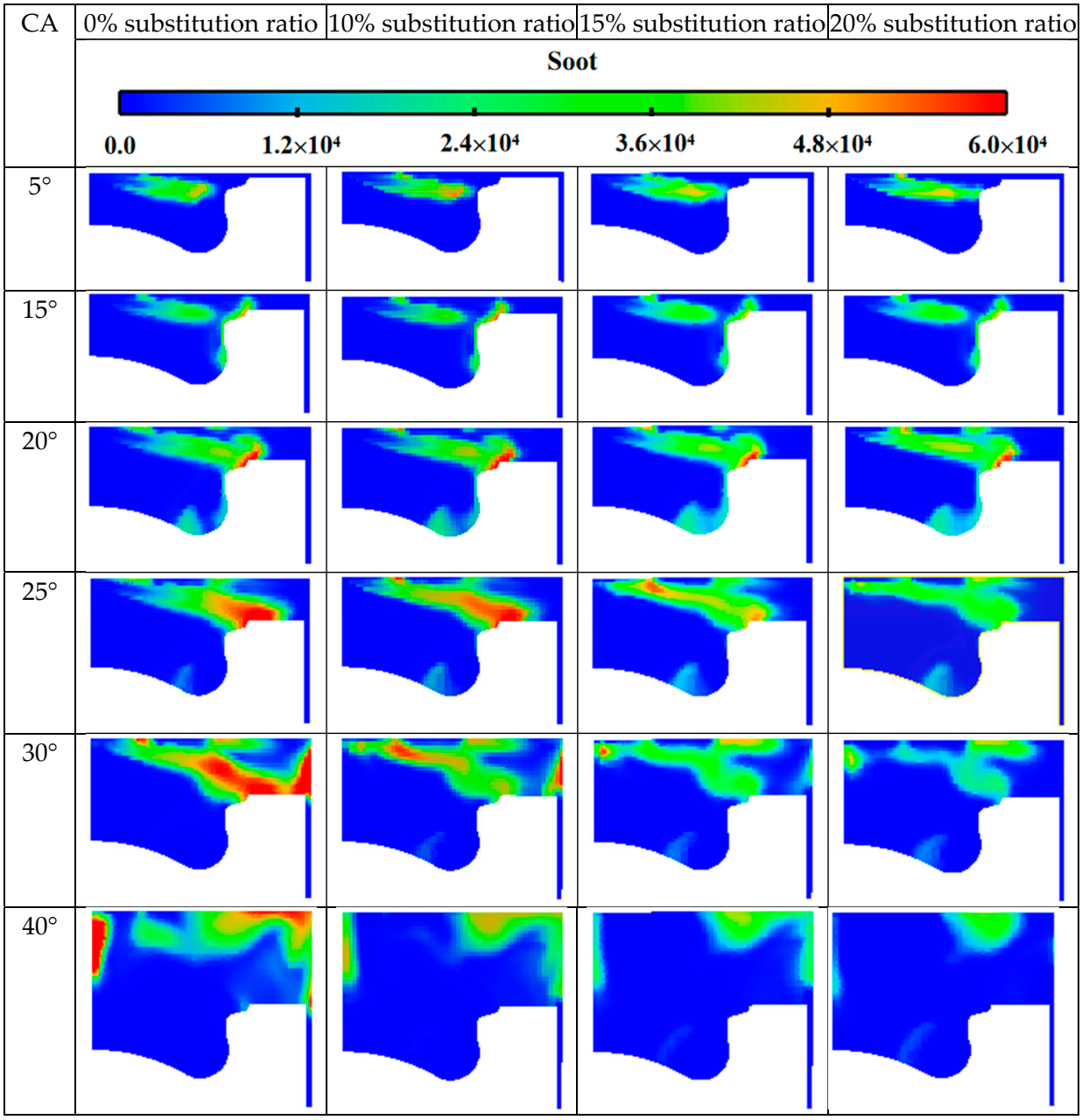

Figure A4. Effects of different DMG substitution ratios on the soot distribution in mass.

Table A1. The initial in-cylinder composition for 15% DMG and different EGR rates.

EGR Rate	O_2 Mass Fraction	N_2 Mass Fraction	H_2 Mass Fraction	CO Mass Fraction	CH_3OH Mass Fraction	H_2O Mass Fraction	CO_2 Mass Fraction
0%	22.648%	75.821%	0.0793%	0.612%	0.840%	0%	0%
10%	21.017%	75.481%	0.0793%	0.612%	0.840%	0.701%	1.403%
20%	19.386%	75.141%	0.0793%	0.612%	0.840%	1.269%	2.539%

References

1. Antunes, J.G.; Mikalsen, R.; Roskilly, A.P. An experimental study of a direct injection compression ignition hydrogen engine. *Int. J. Hydrogen Energy* **2009**, *34*, 6516–6522. [CrossRef]
2. Mohammadi, A.; Shioji, M.; Nakai, Y.; Ishikura, W.; Tabo, E. Performance and combustion characteristics of a direct injection SI hydrogen engine. *Int. J. Hydrogen Energy* **2007**, *32*, 296–304. [CrossRef]

3. Ghazal, O.H. Performance and combustion characteristic of CI engine fueled with hydrogen enriched diesel. *Int. J. Hydrogen Energy* **2013**, *38*, 15469–15476. [CrossRef]
4. Qin, Z.; Yang, Z.; Jia, C.; Duan, J.; Wang, L. Experimental study on combustion characteristics of diesel–hydrogen dual-fuel engine. *J. Therm. Anal. Calorim.* **2020**, *142*, 1483–1491. [CrossRef]
5. Liew, C.; Li, H.; Nuszkowski, J.; Liu, S.; Gatts, T.; Atkinson, R.; Clark, N. An experimental investigation of the combustion process of a heavy-duty diesel engine enriched with H2. *Int. J. Hydrogen Energy* **2010**, *35*, 11357–11365. [CrossRef]
6. Miyamoto, T.; Hasegawa, H.; Mikami, M.; Kojima, N.; Kabashima, H.; Urata, Y. Effect of hydrogen addition to intake gas on combustion and exhaust emission characteristics of a diesel engine. *Int. J. Hydrogen Energy* **2011**, *36*, 13138–13149. [CrossRef]
7. Kumar, M.; Tsujimura, T.; Suzuki, Y. NOx model development and validation with diesel and hydrogen/diesel dual-fuel system on diesel engine. *Energy* **2018**, *145*, 496–506. [CrossRef]
8. Ramsay, C.J.; Dinesh, K.R.; Fairney, W.; Vaughan, N. A numerical study on the effects of constant volume combustion phase on performance and emissions characteristics of a diesel-hydrogen dual-fuel engine. *Int. J. Hydrogen Energy* **2020**, *45*, 32598–32618. [CrossRef]
9. Loganathan, M.; Velmurugan, A.; Page, T.; Gunasekaran, E.J.; Tamilarasan, P. Combustion analysis of a hydrogen-diesel fuel operated DI diesel engine with exhaust gas recirculation. *Front. Energy* **2017**, *11*, 568–574. [CrossRef]
10. Nag, S.; Sharma, P.; Gupta, A.; Dhar, A. Experimental study of engine performance and emissions for hydrogen diesel dual fuel engine with exhaust gas recirculation. *Int. J. Hydrogen Energy* **2019**, *44*, 12163–12175. [CrossRef]
11. Wu, H.W.; Hsu, T.T.; He, J.Y.; Fan, C.M. Optimal performance and emissions of diesel/hydrogen-rich gas engine varying intake air temperature and EGR ratio. *Appl. Therm. Eng.* **2017**, *124*, 381–392. [CrossRef]
12. Talibi, M.; Hellier, P.; Ladommatos, N. The effect of varying EGR and intake air boost on hydrogen-diesel co-combustion in CI engines. *Int. J. Hydrogen Energy* **2017**, *42*, 6369–6383. [CrossRef]
13. Hosseini, S.E.; Wahid, M.A. Hydrogen production from renewable and sustainable energy resources: Promising green energy carrier for clean development. *Renew. Sustain. Energy Rev.* **2016**, *57*, 850–866. [CrossRef]
14. Chuahy, F.D.; Kokjohn, S.L. High efficiency dual-fuel combustion through thermochemical recovery and diesel reforming. *Appl. Energy* **2017**, *195*, 503–522. [CrossRef]
15. Sittichompoo, S.; Nozari, H.; Herreros, J.M.; Serhan, N.; da Silva, J.A.M.; York, A.P.E.; Millington, P.; Tsolakis, A. Exhaust energy recovery via catalytic ammonia decomposition to hydrogen for low carbon clean vehicles. *Fuel* **2021**, *285*, 119111. [CrossRef]
16. Jiang, Y.; Chen, Y.; Xie, M. Effects of blending dissociated methanol gas with the fuel in gasoline engine. *Energy* **2022**, *247*, 123494. [CrossRef]
17. Sahoo, B.B.; Sahoo, N.; Saha, U.K. Effect of H2: CO ratio in syngas on the performance of a dual fuel diesel engine operation. *Appl. Therm. Eng.* **2012**, *49*, 139–146. [CrossRef]
18. Bhaduri, S.; Contino, F.; Jeanmart, H.; Breuer, E. The effects of biomass syngas composition, moisture, tar loading and operating conditions on the combustion of a tar-tolerant HCCI (Homogeneous Charge Compression Ignition) engine. *Energy* **2015**, *87*, 289–302. [CrossRef]
19. Christodoulou, F.; Megaritis, A. Experimental investigation of the effects of simultaneous hydrogen and nitrogen addition on the emissions and combustion of a diesel engine. *Int. J. Hydrogen Energy* **2014**, *39*, 2692–2702. [CrossRef]
20. Karimkashi, S.; Kahila, H.; Kaario, O.; Larmi, M.; Vuorinen, V. Numerical study on tri-fuel combustion: Ignition properties of hydrogen-enriched methane-diesel and methanol-diesel mixtures. *Int. J. Hydrogen Energy* **2020**, *45*, 4946–4962. [CrossRef]
21. Chuahy, F.D.; Kokjohn, S.L. Effects of reformed fuel composition in "single" fuel reactivity controlled compression ignition combustion. *Appl. Energy* **2017**, *208*, 1–11. [CrossRef]
22. Curran, H.J.; Fisher, E.M.; Glaude, P.A.; Marinov, N.M.; Pitz, W.J.; Westbrook, C.K.; Layton, D.W.; Flynn, P.F.; Durrett, R.P.; Zur Loye, A.O.; et al. Detailed chemical kinetic modeling of diesel combustion with oxygenated fuels. *SAE Trans.* **2001**, *110*, 514–521.
23. Hernandez, J.J.; Sanz-Argent, J.; Benajes, J.; Molina, S. Selection of a diesel fuel surrogate for the prediction of auto-ignition under HCCI engine conditions. *Fuel* **2008**, *87*, 655–665. [CrossRef]
24. Liu, Y.D.; Jia, M.; Xie, M.Z.; Pang, B. Enhancement on a skeletal kinetic model for primary reference fuel oxidation by using a semidecoupling methodology. *Energy Fuels* **2012**, *26*, 7069–7083. [CrossRef]
25. Hiroyasu, H.; Kadota, T. Models for combustion and formation of nitric oxide and soot in direct injection diesel engines. *SAE Trans.* **1976**, *85*, 513–526.
26. Mellor, A.M.; Mello, J.P.; Duffy, K.P.; Easley, W.L.; Faulkner, J.C. Skeletal Mechanism for NOx Chemistry in Diesel Engines. *SAE Trans.* **1998**, *107*, 786–801.
27. Zhu, Y.; Jia, M.; Niu, B.; Tian, J.; Li, H.; Fan, J. Development of diesel surrogates for reproducing the effect of fuel properties on engine combustion and emissions using an optimized decoupling physical–chemical surrogate (DPCS) model. *Fuel* **2022**, *310*, 122424. [CrossRef]
28. Li, Y.; Jia, M.; Liu, Y.; Xie, M. Numerical study on the combustion and emission characteristics of a methanol/diesel reactivity controlled compression ignition (RCCI) engine. *Appl. Energy* **2013**, *106*, 184–197. [CrossRef]

Disclaimer/Publisher's Note: The statements, opinions and data contained in all publications are solely those of the individual author(s) and contributor(s) and not of MDPI and/or the editor(s). MDPI and/or the editor(s) disclaim responsibility for any injury to people or property resulting from any ideas, methods, instructions or products referred to in the content.